Cuffe, C., Attree, E., Clark, E., Piercy, R., Psifidi, A. (2026) The epigenetic and transcriptional signatures of oxidative versus glycolytic muscles in horses, *Proceedings 13th World Congress on Genetics Applied to Livestock Production*:24116 https://doi.org/10.31274/wcgalp.24116
©2026 *Cuffe, et al.* CC BY-NC-ND

The epigenetic and transcriptional signatures of oxidative versus glycolytic muscles in horses

C. Cuffe[1*], E. Attree[1], E. Clark[2,3], R.J. Piercy[1], A. Psifidi[1,2]

[1]The Royal Veterinary College, Hatfield, UK. [2]The Roslin Institute, The Royal (Dick) School of Veterinary Studies, University of Edinburgh, Scotland, UK [3]European Bioinformatics Institute, Hinxton, UK; [*]Corresponding author: ccuffe22@rvc.ac.uk

Introduction

Mature equine skeletal muscles are composed of varying proportions of three different fibre types: type 1 - slow twitch oxidative, type 2A - fast twitch oxidative and type 2X - fast twitch glycolytic. In muscle-fibres fast or slow twitch refers to the maximal shortening velocities of the fibre, while oxidative or glycolytic refers to the primary energy pathway used to generate ATP. Fibre-type proportion can vary depending on primary muscle function and breed, as well as in response to exercise (Serrano and Rivero 2000; Serrano et al 2000; Hyytiäinen et al 2014). In this study we have compared the semimembranosus (SM) and the sacrocaudalis dorsalis medialis (SCDM), two muscles with different functions in the horse. The SM is a primarily glycolytic locomotor muscle with similar muscles showing over 70% Type 2X fibres (Hyytiäinen et al 2014). In comparison the SCDM is a primarily oxidative muscle with a largely stabilising function. Muscles with a largely stabilising or postural function such as the SCDM are enriched in Type 1 muscles, with Hyytiäinen et al (2014) demonstrating that SCDM is enriched with over 80% type 1 fibres.

These muscles are also of interest for diagnostic reasons. For example, the SCDM is biopsied in cases where equine motor neurone disease is suspected, and the SM is biopsied to diagnose exertional rhabdomyolysis or polysaccharide storage myopathy (Ledwith and McGowan 2004). In this study we aim to characterise and compare the two different types of muscles at the epigenetic and transcriptional level to improve our understanding and support future research on equine myopathies.

Materials & Methods

This work was done with full ethical approval from the RVC's CRERB, under the following URN: 2023 2203-2. Samples from 6 thoroughbreds (TB) and 6 warmbloods (WB) were used and collected prior to the commencement of this study. WB samples were collected for clinical reasons following owner requested euthanasia, while TB samples were collected from horses maintained and euthanised under ASPA licence PED82E67D. For both breeds the average age was seven years old, with the TB samples having a range of three to ten years and the WB's having a range of six to ten years. For each animal, samples from the SM and the SCDM were collected and preserved in triplicate. One sample was adhered to a cork disk with optimal cutting temperature compound (OCT) and flash frozen in isopentane, cooled in liquid nitrogen, to be used for the immunohistochemistry (IHC), then the remaining sample was split between cryovials containing RNAlater for RNA-seq or had nuclei extracted with a dounce homogeniser and cryopreserved in a DMSO-sucrose buffer for ATAC-seq. All samples were used for the RNA-sequencing work, a subset of three WBs and three TBs were used for the IHC. Finally for the assay for transposase accessible sequencing (ATAC-seq) two TBs had SM and SCDM sequenced, two had only the SCDM sequenced and two had only the SM. For the WBs, four had both sequenced and one had only the SCDM sequenced.

Immunohistochemistry was used to quad label 8µm sections of the frozen muscle with collagen, and myosin heavy chain isoforms corresponding to type 1 fibres, type 2a fibres and to myosin

heavy chain fast fibres (all type 2 fibres) as described (Tulloch and Perkins et al 2011). The fibre-type proportions were calculated for three images per muscle per horse, images were taken at 10x magnification on a Nikon Eclipse Ni-E (Amstelveen, The Netherlands) this was done with the aid of cell-counter in ImageJ.
For ATAC-seq library preparation, the samples were defrosted in 10ml PBS and underwent two rounds of filtering at 0.70µm and 0.40µm. Nuclei were counted using Trypan Blue and 100,000-150,000 nuclei were used for ATAC-Seq library prep. This was done using the ATAC-seq kit, cat: 53150, from Active Motif (California, USA), ATAC-Seq libraries were sent to Novogene for sequencing at a depth of ~ 100 million reads per sample, 150bp paired end.
For the RNA-seq, ~30mg of RNAlater preserved sample was minced with a scalpel, underwent homogenisation in a Fastprep96 (MP Biomedicals, California, USA) with 10µl β-mercaptoethanol, 1ml trizol and a steel bead in three rounds of bead beating at 1200 rpm for 30s. Next 300µl of chloroform was added and centrifuged for 15 minutes at 4˚C (LX-165T2R benchtop microcentrifuge, Haier Biomedical, Surrey, UK). The upper clear aqueous phase was transferred to a new 1.5ml tube and 500 µl isopropanol was added, centrifuged again and then this was input into the spin columns from the Qiagen RNAeasy extraction kit (Qiagen, Hilden, Germany). An additional DNase 1 treatment (Qiagen, Hilden, Germany) was performed before the final washes. Quality for both ATAC libraries and extracted RNA was checked using a DS-C spectrophotometer (deNovix, Wilmington, USA), Qubit 4 (Invitrogen, Waltham, USA) and Tapestation 4150 system (Agilent, Santa Clara, USA). The extracted RNA was sequenced at 150bp paired end with ~60 million reads per sample by Novogene.
RNA-seq samples were analysed using the NF-core RNA-seq pipeline (3.14.0) (Patel et al 2025). Briefly reads were aligned using STAR (Dobin et al, 2013) to EquCab3.0, with transcripts quantified using salmon (Patro et al 2017). Differentially expressed genes (DEGs) were identified using DESeq2 (Love et al 2014), including the following covariates within the model; breed, age and sequencing batch. Significant DEGs were those with an FDR adjusted p-value < 0.05, and a $\log_2$foldchange >1 or <-1. The DAVID database (Sherman et al 2022) was used for functional annotation clustering analysis of the DEGs, where clusters with an enrichment score above 1.5 were considered significant. Functional annotation was performed to provide further insights into the pathways involved in the regulation of different muscle types. This analysis was done both across breed and within breed. ATAC-seq reads were aligned using BWA-mem (Li 2013) with the EquCab3.0 genome, quality filtered for low quality reads, mitochondrial reads and those mapping to unassigned contigs. Then the samples were merged across all SM and all SCDM replicates. Peaks were called with MACS2 (Zhang et al 2008) before TOBIAS (Bentsen et al 2020) was used to identify transcription factor binding sites and differential binding from aggregate peaks. These results were integrated to aid in our understanding of the regulatory differences between the SM and SCDM.

Results & Discussion

Immunohistochemistry confirmed fibre-type proportions for our samples, with the SCDM samples having ~75% type 1 oxidative fibres, and 2% type 2X glycolytic fibres, compared to the SM with ~ 12% type 1 fibres and 49% type 2X fibres, (**Error! Reference source not found.**). SCDM fibre-type proportions are similar to those seen in the literature, with a mean type 1 proportion of 84% and 4.5% type 2X (Hyytiäinen et al 2014), while SM have previously shown 15% type 1 fibres and 35% type 2X fibres (Serrano et al 2000).

RNA-seq analysis comparing the two types of muscle identified 737 DEGs. Of these 737 genes, 415 were long non-coding RNA (lncRNA), 319 were protein coding. Functional enrichment analyses showed enrichment for biological processes involved in glycolytic processes-ADP/ATP metabolic processes, and actin binding.

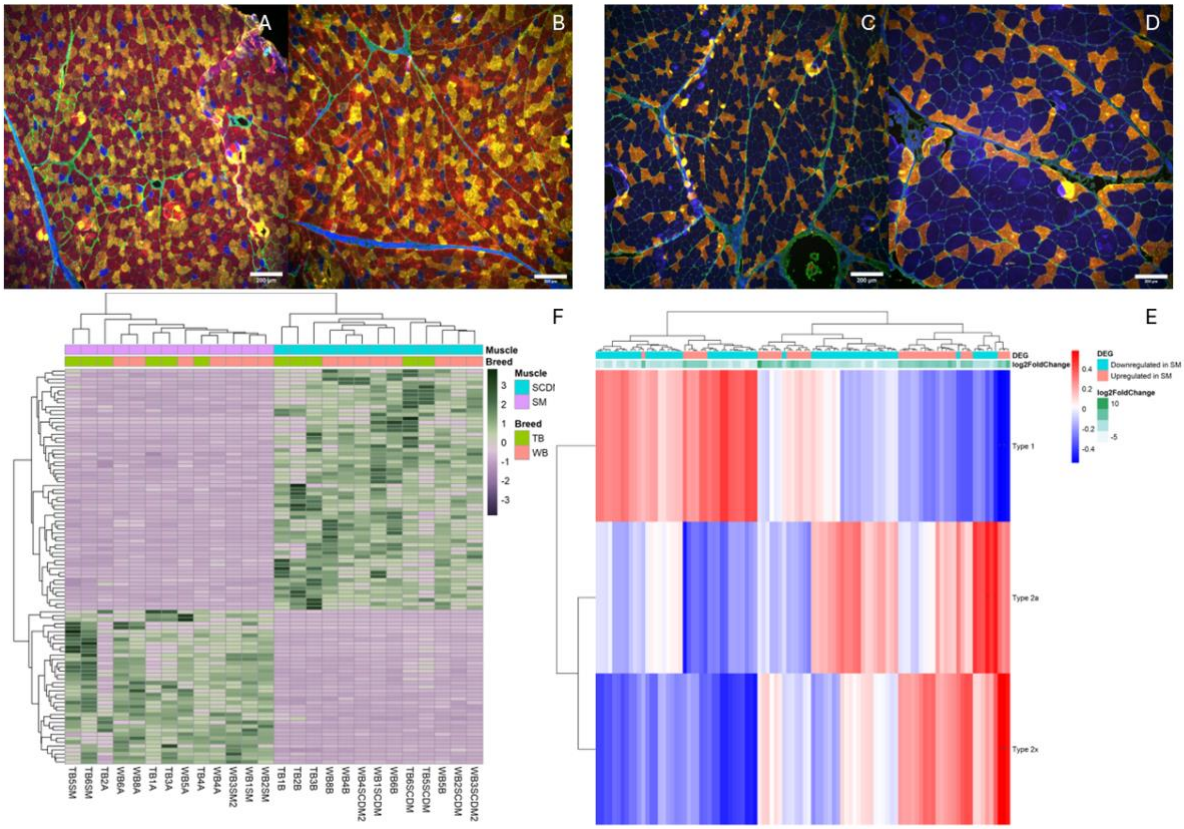

Figure 1. Images from frozen muscle sections labelled by IHC for fibre-type and collagen. Blue is type 1, red is type 2X, orange/yellow is type 2A, and green is collagen. Images are taken at 10x magnification on a Nikon Ni-E.. A & B show images from the SM, with a thoroughbred sample in A and a warmblood in B. While C & D show an example SCDM from the same thoroughbred in C and warmblood in D. The scale bar in each image represents 200 µm. E Shows the correlation of the top 100 DEGs with fibre-type proportions for a subset of the animals. Heatmap is coloured based on a Pearson correlation between gene expression and fibre type, with Log2FoldChange shown above the plot and DEG showing upregulated genes in the SM in blue and downregulated genes in orange. F shows a heatmap from the RNA-seq with the top 100 DEGs showing distinct clustering by muscle type, SM in purple and SCDM in blue. Heatmap is coloured based on a z-score showing relative expression differences per gene.

Using the fibre-type proportions of a subset of animals we were able to correlate individual gene expression to fibre-type proportion, these correlations were used for the heatmap seen in Figure 1E. Here you can see that the correlations seem broadly similar between type 2A and type 2X fibres, with largely inverse correlations seen with the type 1 fibres. The clustering of type 2A and type 2X is likely due to similarities in the genes enriched by myosin heavy chain fast fibres versus the slow myosin heavy chain isoform seen in type 1 fibres. As seen in Figure 1F the genes clustered according to muscle, with some breed clustering seen next. DAVID results highlighted a single over enriched pathway, GO:0006096~glycolytic process (17.75-fold enrichment, 1.86 E-3 FDR). The identified top 20 DEGs by adjusted p value, were further investigated by functional enrichment using PANTHER (Mi et al, 2019). This group of genes were identified to have roles in skeletal system development, actin polymerisation, carbohydrate metabolism and glucogenesis along with regulation of angiogenesis and blood vessel modelling.

ATAC-seq analysis using TOBIAS identified 233 transcription factors (TFs), that were significantly differentially bound between the two types of muscles. Using the aggregate peak files for SM or SCDM samples, peaks were annotated with genes where the promotor region

overlapped. Promotor regions were regions up to 5kb downstream of transcription start sites and 3kb upstream. From this only 0.8% of genes had promoter regions located solely within SM peaks, while 14% were located within SCDM peaks, however the majority were overlapped by peaks in both muscles (1439 protein-coding genes). Analysis of differential TF binding revealed two associated pathways involved in JAK-STAT signalling and the apelin signalling pathway as being slightly over enriched. In mice apelin knockouts have shown a decrease in myofiber size due to an increase in type 1 fibres, alongside a downregulation of glucose metabolism related genes (Kilpiö et al 2024). The JAK-STAT signalling pathway has the incongruent roles in skeletal muscle of promoting muscle hypertrophy and muscle atrophy, regulated by histone acetylation and methylation (Moresi et al 2019), highlighting the importance of gene regulation in muscle development and fibre-type differentiation.

Conclusions

In conclusion this study highlighted significant differences in gene expression and regulation of glycolytic versus oxidative muscles. Cell apoptosis, glucose metabolism and gene regulation were key processes differentiating SM and SCDM muscles. This study provides a baseline for comparison of different muscles and a foundation for future research into equine myopathies.

Acknowledgements

We greatly appreciate the help of colleagues at the comparative neuromuscular diseases lab for their help with this work. We also thank our funders the Paul Mellon Fund and Horserace betting levy board.

References

Serrano, A.L., J.L.L. Rivero (2000) J. Muscle Res. & Cell Motility 21:235. doi.org/10.1023/A:1005642632711.
Serrano, A.L., E. Quiroz-Rothe, J.L. Rivero (2000) Pflugers Archiv: European Journal of Physiology 441(2–3):263–274. doi.org/10.1007/s004240000408.
Hyytiäinen, H.K., A.K. Mykkänen, A.K. Hielm-Björkman, N.C. Stubbs, C.M. McGowan (2014) Acta Veterinaria Scandinavica 56(1):8. doi.org/10.1186/1751-0147-56-8.
Ledwith, A., C.M. McGowan (2004) Equine Vet. Educ. 16(2):62. doi.org/10.1111/j.2042-3292.2004.tb00268.x.
Tulloch, L.K., J.D. Perkins, R.J. Piercy (2011) Equine Vet. J. 43:500. doi.org/10.1111/j.2042-3306.2010.00329.x.
Patel, H., J. Manning, P. Ewels, M.U. Garcia, A. Peltzer, et al, nf-core/rnaseq: nf-core/rnaseq v3.22.2 - Perfect Palladium Penguin. Available at: https://zenodo.org/records/17909656, visited on: 19-January-2026.
Dobin, A., C.A. Davis, F. Schlesinger, J. Drenkow, C. Zaleski, et al (2013) Bioinformatics (Oxford, England) 29(1):15–21. doi.org/10.1093/bioinformatics/bts635.
Patro, R., G. Duggal, M.I. Love, R.A. Irizarry, C. Kingsford (2017) Nat. Meth. 14:417. doi.org/10.1038/nmeth.4197.
Love, M.I., W. Huber, S. Anders (2014) Genome Biology 15(12):550. doi.org/10.1186/s13059-014-0550-8.
Sherman, B.T., M. Hao, J. Qiu, X. Jiao, M.W. Baseler, H.C. Lane, T. Imamichi, W. Chang (2022) Nucleic Acids Research 50(W1):W216–W221. doi.org/10.1093/nar/gkac194.
Li, H., Aligning sequence reads, clone sequences and assembly contigs with BWA-MEM. arXiv:1303.3997v1 [q-bio.GN].
Zhang, Y., T. Liu, C.A. Meyer, J. Eeckhoute, D.S. Johnson, et al (2008) Genome Biology 9(9):R137. doi.org/10.1186/gb-2008-9-9-r137.
Bentsen, M., P. Goymann, H. Schultheis, K. Klee, A. Petrova, et al (2020) Nat. Comm. 11(1):4267. doi.org/10.1038/s41467-020-18035-1.
Mi, H., A. Muruganujan, X. Huang, D. Ebert, C. Mills, X. Guo, P.D. Thomas (2019) Nature Protocols 14(3):703–721. doi.org/10.1038/s41596-019-0128-8.
Kilpiö, T., S. Skarp, Á. Perjés, J. Swan, L. Kaikkonen, et al (2024) American Journal of Physiology. Cell Physiology 326(5):C1437–C1450. doi.org/10.1152/ajpcell.00427.2023.
Moresi, V., S. Adamo, L. Berghella (2019) Frontiers in Physiology 10: doi.org/10.3389/fphys.2019.00500.